

Zinc oxide-chitosan nanobiocomposite for urea sensor

Pratima R. Solanki,^{a)} Ajeet Kaushik, Anees A. Ansari, G. Sumana, and B. D. Malhotra^{a)}
*Biomolecular Electronics & Conducting Polymer Research Group, National Physical Laboratory,
 Dr. K. S. Krishnan Marg, New Delhi 110012, India*

(Received 31 July 2008; accepted 20 August 2008; published online 24 October 2008)

Zinc oxide (ZnO)-chitosan (CH) nanobiocomposite film onto indium-tin-oxide (ITO) coated glass has been used to immobilize urease (Urs) and glutamate dehydrogenase (GLDH) for urea detection. The presence of ZnO nanoparticles in CH results in its increased surface area and enhanced electron transfer kinetics. The Urs-GLDH/CH-ZnO/ITO bioelectrode characterized using electrochemical, Fourier transform infrared, and scanning electron microscopy studies exhibit linearity of 5–100 mg/dl, detection limit of 3 mg/dl, response time of 10 s, reproducibility as 20 times, and shelf life of 3 months. The low Michaelis–Menten constant (K_m) value (4.92 mg/dl) indicates enhanced affinity of enzyme with nanobiocomposite. © 2008 American Institute of Physics. [DOI: 10.1063/1.2980448]

Estimation of urea in serum/blood/urine is important for diagnosis of renal and liver diseases. An increase in urea level (normal range is 8–20 mg/dl) in blood and urine causes renal failure, urinary tract obstruction, dehydration, shock, burns, and gastrointestinal bleeding. Moreover, reduced urea level may cause hepatic failure, nephritic syndrome, and cachexia (low-protein and high-carbohydrate diets).

Most urea biosensors based on urease (Urs) are based on catalytic conversion of urea to hydrogen bicarbonate and ammonium.^{1–3} It has been observed that ammonium ions easily diffuse in solution. Thus, glutamate dehydrogenase^{4,5} (GLDH) has been used as an alternate since it catalyzes the reaction between ammonium ions, α -ketoglutarate (α -KG) and nicotinamide adenine dinucleotide (NADH) to produce L-glutamate and NAD^+ .

The immobilization of Urs on a given matrix is a crucial step for the fabrication of urea biosensor. Extensive efforts have been made to utilize nanomaterials to immobilize Urs for urea detection. Among nanostructured metal oxides such as cerium oxide (CeO_2),⁶ tin oxide (SnO_2), and zirconium oxide (ZrO_2)⁷ nanoparticles etc., zinc oxide (ZnO)⁸ nanoparticles have been used for fabrication of transducer surface because of their unique ability to promote faster electron transfer between electrode and active site of desired enzyme. This has been attributed to their remarkable properties such as wide band gap (3.37 eV), high surface area, high catalytic efficiency, nontoxicity, chemical stability, strong adsorption ability [high isoelectric point (IEP) \sim 9.5],⁹ and for immobilization of low IEP (\sim 5.0) proteins via electrostatic interactions. ZnO nanoparticles have recently been used for direct adsorption and interaction of desired enzymes with ZnO nanoparticles. The biocompatible ZnO nanoparticles have unique advantages for enzyme immobilization due to desirable microenvironment for enhanced direct electron transfer between enzyme's active sites and the electrode.^{10,11} However, biosensing properties of ZnO nanoparticles can be improved by incorporating these in chitosan (CH) to prepare ZnO-CH hybrid nanobiocomposite.¹² CH exhibits excellent film forming ability, nontoxicity, and biocompatibility has

led to growing interest for immobilization of biomolecules. Moreover, presence of amine and hydroxyl group in CH helps in the immobilization of desired enzyme.^{13–15} Recently, ZnO-CH nanobiocomposite films have been proposed for amperometric immunosensor for human IgG. Moreover, ZnO-CH composite film can be used for application to H_2O_2 , phenol and cholesterol biosensor, respectively.¹⁶ However, no attempts have been made towards application of ZnO-CH nanobiocomposite film to urea detection.

We report results of studies relating to immobilization of Urs-GLDH onto ZnO-CH nanobiocomposite film deposited onto indium-tin-oxide (ITO) glass substrate for fabrication of urea sensor.

ZnO nanoparticles (5 mg) prepared using coprecipitation method¹⁷ were dispersed into CH solution (50 mg of CH was dissolved in 10 ml of 0.05M acetate buffer) with stirring at room temperature followed by sonication for about 1 h. The ZnO nanoparticles film (200 nm) was spin-cast onto ITO glass with speed of 3000 rpm and allowed to dry at room temperature (25 °C). This ZnO-CH/ITO electrode was rinsed with phosphate buffer (50 mM, pH 7.0) to neutralize the matrix.

The solution containing Urs (10 mg/ml) and GLDH (1 mg/ml) in 1:1 ratio in phosphate buffer (50 mM, pH 7.0) was immobilized onto ZnO-CH/ITO nanobiocomposite electrode by physisorption technique via electrostatic interactions between matrix and enzyme. The Urs-GLDH/ZnO-CH/ITO bioelectrode is kept undisturbed for about 12 h at 4 °C. Finally, the dry bioelectrode is immersed in 50 mM PBS (pH 7.0) in order to wash out any unbound enzyme from the electrode surface.

X-ray diffraction (XRD), (Rigaku) studies have been done to identify the crystal structure of ZnO powder. Scanning electron microscopy (SEM) (LEO-440) studies have been conducted to examine surface morphologies of ZnO-CH/ITO nanobiocomposite and Urs-GLDH/ZnO-CH/ITO bioelectrodes. Electrochemical analysis has been conducted on an Autolab Potentiostat/ Galvanostat (Eco Chemie, Netherlands) using a three-electrode system with ITO as working electrode (0.25 cm^2), platinum wire as the auxiliary electrode and Ag/AgCl electrode as reference electrode in phosphate buffer saline (PBS), (50 mM, pH 7.0, 0.9% NaCl) containing 5 mM $[\text{Fe}(\text{CN})_6]^{3-/4-}$.

^{a)}Tel.: +91-11-45609152 FAX: +91-11-45609310. Electronic addresses: pratimasolanki@yahoo.com and bansi.malhotra@gmail.com.

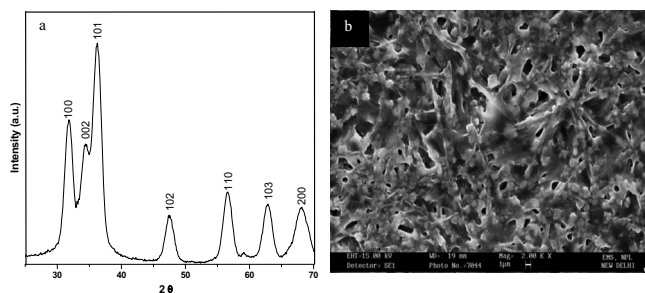


FIG. 1. (a) XRD pattern of ZnO-CH nanobiocomposite film. (b) SEM of Urs-GLDH/ZnO-CH/ITO bioelec-trode.

Figure 1(a) shows XRD pattern carried out on ZnO powder sample. The x-ray diffractograms (in the range 2θ , 30° – 70°) of the film show presence of (100), (002), (101), (102), (110), (103), and (200) reflection planes corresponding to hexagonal wurtzite structure of ZnO.¹⁷ However, broadening in reflection planes indicates nanocrystalline nature of particles. The average crystallite size of ZnO nanoparticles estimated according to Scherrer's formula is 4–5 nm.

Fourier transform infrared (FTIR) spectra (data not shown) of ZnO-CH nanobiocomposite exhibits infrared bands corresponding to ZnO nanoparticles and pure CH, indicating that $-\text{NH}_2$ and $-\text{OH}$ groups of CH due to complex formation resulting in enhanced accumulation ability of ZnO nanoparticles and electrocatalytic activity of ZnO-CH nanobiocomposite film. However, shapes of the absorption peaks of ZnO-CH nanobiocomposite become broader due to overlapping of the functional groups of Ur-GLDH and ZnO-CH nanobiocomposite film indicating immobilization of Ur-GLDH onto nanobiocomposite matrix.

SEM image of ZnO-CH/ITO nanobiocomposite shows cage like morphology indicating uniform dispersion of ZnO nanoparticles into CH (data not shown). SEM image of Urs-GLDH/ZnO-CH [Fig. 1(b)] reveals that enzymes (Urs-GLDH) are present uniformly distributed in ZnO-CH composite. The uniform dispersion of Urs-GLDH reveals that enzyme binds with $-\text{NH}_2$ and $-\text{OH}$ terminal of CH via electrostatic interactions. Moreover, positively charged ZnO-CH nanobiocomposite due to CH and ZnO (IEP ~ 9.5) results in electrostatic interactions with negatively charged Urs-GLDH (IEP of 5.0–5.3 at pH 7.0).

Figure 2(a) shows electrochemical impedance spectra (EIS, Nyquist plot) of CH/ITO electrode (curve i), ZnO-CH/ITO electrode (curve ii), and Urs-GLDH/ZnO-CH/ITO bio-

electrode (curve iii). In the EIS, the semicircle diameter is equal to electron-transfer resistance R_{CT} . The R_{CT} of CH decreases from 3.27 to 2.04 k Ω after incorporation of ZnO nanoparticles, indicating that ZnO nanoparticles result in enhanced electron transfer kinetics on nanobiocomposite electrode. After immobilization of Urs-GLDH onto ZnO-CH nanobiocomposite, R_{CT} increases to 9.47 k Ω revealing immobilization of Urs-GLDH onto ZnO-CH/ITO matrix resulting in blocking of charge carriers in the nanobiocomposite. The variations of solution resistance (R_s), double layer capacitance (C_{dl}), and Warburg element (Z_W) are shown in Fig. 2(a).

Figure 2(b) shows cyclic voltammograms of CH/ITO electrode, ZnO-CH/ITO electrode, and Urs-GLDH/ZnO-CH/ITO bioelectrode. It is observed that magnitude of peak current slightly decreases and peak potential shifts toward lower potential ($E_{pa} \sim 0.23$ V) as compared to that of CH/ITO electrode. The decrease of peak current and shift of the oxidation peak potential of ZnO-CH/ITO electrode may be attributed to faster electron transfer in ZnO-CH nanobiocomposite. Further, redox current of Urs-GLDH/ZnO-CH/ITO bioelectrode is found to decrease due to insulating characteristics of Urs-GLDH indicating slow down of redox process during the biochemical reaction.

Figure 2(c) shows CVs of Urs-GLDH/ZnO-CH/ITO bioelectrode as a function of scan rate from 10 to 100 mV/s. The proportional increase of redox current with respect to scan rate is observed indicating diffusion-controlled system [inset Fig. 2(c)]. The surface concentration of Urs-GLDH/ZnO-CH/ITO bioelectrode estimated from plot of I_p versus scan rate ($\nu^{1/2}$) using Brown–Anson model has been found to be 3.8×10^{-8} mol cm^{-2} . The diffusion coefficient value (D) of ZnO-CH/ITO electrode has been estimated using Sandel–Sevcik equation

$$I_p = (2.69 \times 10^5) n^{3/2} A D^{1/2} C \nu^{1/2}, \quad (1)$$

where I_p is peak current (I_{pa} anodic and I_{pc} cathodic), n is electron stoichiometry, A is electrode area (0.25 cm^2), D is diffusion coefficient, C is surface concentration ($3.8 \times 10^{-8} \text{ mol cm}^{-2}$), and ν is scan rate (10 V/s). The D value has been obtained as $8.22 \times 10^{-4} \text{ cm}^2 \text{ s}^{-1}$.

Figure 3(a) shows electrochemical response of Urs-GLDH/ZnO-CH/ITO bioelectrode as a function of urea in presence of NADH (30 μl) and α -ketoglutarate (70 μl) studied using CV technique. The magnitude of peak current increases linearly as urea concentration increases (linear range as 5–100 mg/dl). Inset (i) in Fig. 3(a) exhibits linear

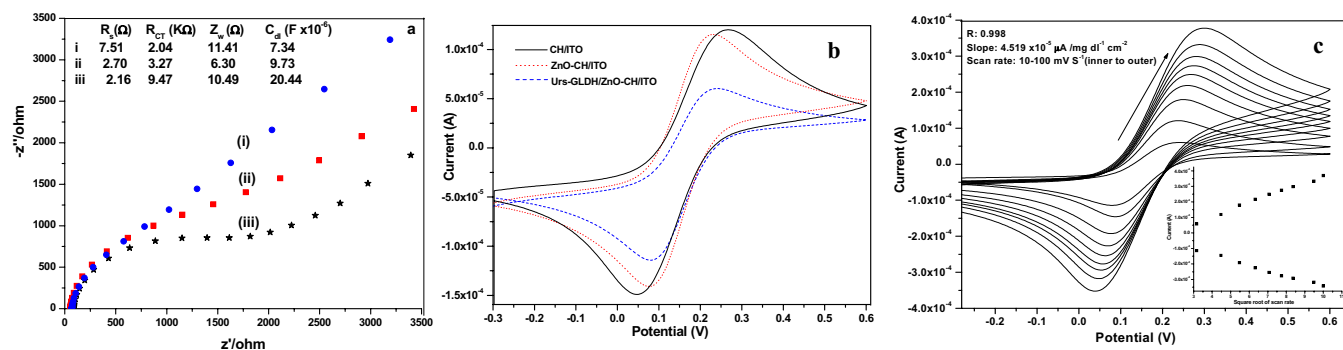


FIG. 2. (Color online) (a) EIS of (i) CH/ITO, (ii) ZnO-CH/ITO electrode, and (iii) Urs-GLDH/ZnO-CH/ITO. (b) Cyclic voltammogram of CH/ITO, ZnO-CH/ITO and Urs-GLDH/ZnO-CH/ITO bioelectrode at 10 mV/s scan rate in PBS containing 5 mM $[\text{Fe}(\text{CN})_6]^{3-/4-}$. (c) CV of Urs-GLDH/ZnO-CH/ITO bioelectrode at different scan rates, 10–100 mV/s.

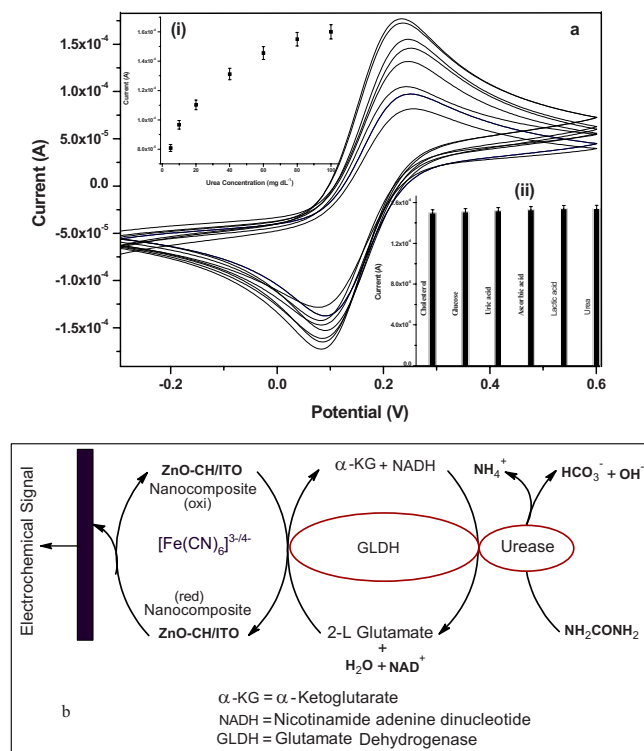


FIG. 3. (Color online) (a) Electrochemical response of Urs-GLDH/ZnO-CH/ITO bioelectrode with respect to urea concentration (5–100 mg dl⁻¹) at scan rate of 10 mV s⁻¹. Inset a: linearity curve between magnitude of current vs urea concentration. Inset b: effect of interferents on Urs-GLDH/ZnO-CH/ITO bioelectrode. (b) The electrochemical reaction at Urs-GLDH/ZnO-CH/ITO bioelectrode.

increase in current as a function of urea concentration. It may be noted that values of electrochemical response current obtained using several Urs-GLDH/ZnO-CH/ITO bioelectrodes are reproducible within 0.1%.

Electrochemical reaction occurring at Urs-GLDH/ZnO-CH/ITO bioelectrode is shown in Fig. 3(b). The Michaelis–Menten constant (K_m) value obtained using Linweaver–Burke equation has been estimated as 4.92 mg/dl (0.82 mM) with sensitivity as 0.13 $\mu\text{A}/\text{mM cm}^2$, linear regression as 0.988, and standard deviation as 9.4 $\mu\text{A}/\text{mg dl}^{-1}$. The lower K_m value reflects higher enzymatic affinity of Urs-GLDH/ZnO-CH/ITO with urea due to biocompatibility, active surface area, and high electron communication capability of ZnO-CH nanobiocomposite.

The detection limit has been estimated as 3 mg/dl using $3\sigma_b/m$ criteria, where m is slope of the calibration graph and σ_b is standard deviation of the blank signal. The reproducibility of response of bioelectrode has been investigated at 10 mg/dl urea concentration. No significant decrease in current is observed after using at least 20 times. This bioelectrode achieves 95% of steady state current in less than 5 s indicating fast electron exchange between Urs-GLDH and ZnO-CH/ITO electrode.

The effect of pH (6.0–8.0 at 25 °C) on Urs-GLDH/ZnO-CH/ITO bioelectrode has been studied using CV to estimate enzyme activity that depends upon the conformation and electrostatic state of the enzyme's active site. The highest current (data not shown) is obtained at pH 7.0 revealing that

bioelectrode is most active at this pH. Thus, all the experiments are carried out at a pH of 7.0 at 25 °C.

The selectivity of Urs-GLDH/ZnO-CH/ITO bioelectrode has been estimated by comparing magnitude of the current response by adding normal concentration of interferents such as glucose (5 mM), ascorbic acid (0.05 mM), uric acid (0.1 mM), cholesterol (5 mM), and lactic acid (5 mM). The role of interferents has been examined by mixing desired interferent in equal concentrations with that of urea and the results are depicted in inset (ii), Fig. 3(a). It has been found that Urs-GLDH/ZnO-CH/ITO bioelectrode is not significantly affected due to presence of these interferents. And the value of the current remains nearly same except for cholesterol wherein there is a decrease of about 5%.

ZnO-CH based nanobiocomposite electrode has been used to immobilize Urs-GLDH to fabricate electrochemical urea biosensor. The Ur-GLDH/ZnO-CH/ITO urea biosensor shows improved characteristics such as linearity as 5–100 mg/dl, low detection limit (3 mg/dl), linear regression as 0.988, standard deviation as 9.4 $\mu\text{A}/\text{mg dl}^{-1}$, response time of 10 s, and shelf life of 3 months. The value of Michaelis–Menten constant (K_m) obtained as 4.92 mg/dl (0.819 mM) indicates high affinity of Urs-GLDH to urea. Efforts should be made to utilize this Urs-GLDH/ZnO-CH/ITO bioelectrode for estimation of urea in serum samples and utilize it for fabrication of other biosensors.

We thank Director, National Physical Laboratory for providing facilities. P.R.S., A.A.A., and A.K. thank CSIR, India for award of Senior Research Associateships and Senior Research Fellowship.

- ¹Rajesh, V. Bisht, W. Takashima, and K. Kaneto, *Biomaterials* **26**, 3683 (2005).
- ²B. Lakard, G. Herlem, S. Lakard, A. Antoniou, and B. Fahys, *Biosens. Bioelectron.* **19**, 1641 (2004).
- ³G. Dhawan, G. Sumana, and B. D. Malhotra, *Biochem. Eng. J.* (unpublished).
- ⁴A. Maaref, H. Barhoumi, M. Rammah, C. Martelet, N. Jaffrezic-Renault, C. Mousty, and S. Counier, *Sens. Actuators B* **123**, 671 (2007).
- ⁵E. J. Sampson, M. A. Baird, C. A. Burtis, E. M. Smith, D. L. Wltte, and D. D. Bayse, *Clin. Chem.* **26**, 816 (1980).
- ⁶A. A. Ansari, P. R. Solanki, and B. D. Malhotra, *Appl. Phys. Lett.* **92**, 263901 (2008).
- ⁷H. J. Kim, S. H. Yoon, H. N. Choi, Y. K. Lyu, and W. Y. Lee, *Bull. Korean Chem. Soc.* **27**, 65 (2006).
- ⁸S. P. Singh, S. K. Arya, P. Pandey, B. D. Malhotra, S. Saha, K. Sreenivas, and V. Gupta, *Appl. Phys. Lett.* **91**, 063901 (2007).
- ⁹J. X. Wang, X. W. Sun, A. Wei, Y. Lei, X. P. Cai, C. M. Li, and Z. L. Dong, *Appl. Phys. Lett.* **88**, 233106 (2006).
- ¹⁰S. Krishnamoorthy, T. Bei, E. Zoumakis, G. P. Chrousos, and A. Iliadis, *Biosens. Bioelectron.* **22**, 707 (2006).
- ¹¹A. Wei, X. W. Sun, J. X. Wang, Y. Lei, X. P. Cai, C. M. Li, Z. L. Dong, and W. Huang, *Appl. Phys. Lett.* **89**, 123902 (2006).
- ¹²R. Khan, A. Kaushik, P. R. Solanki, A. A. Ansari, M. K. Pandey, and B. D. Malhotra, *Anal. Chim. Acta* **616**, 207 (2008).
- ¹³J. Cruz, M. Kawasaki, and W. Gorski, *Anal. Chem.* **72**, 680 (2000).
- ¹⁴Y. Miao and S. N. Tan, *Analyst (Cambridge, U.K.)* **125**, 1591 (2000).
- ¹⁵C. Xu, H. Cai, P. He, and Y. Fang, *Analyst (Cambridge, U.K.)* **126**, 62 (2001).
- ¹⁶Y. L. Liu, Y. H. Yang, H. F. Yang, Z. M. Liu, G. L. Shen, and R. Q. Yu, *J. Inorg. Biochem.* **99**, 2046 (2005).
- ¹⁷A. Kaushik, J. Kumar, K. K. Tiwari, R. Khan, B. D. Malhotra, V. Gupta, and S. P. Singh, *J. Nanosci. Nanotechnol.* **8**, 1757 (2008).